Microstructures and Properties of Unirradiated and Irradiated High-Strength Invar Alloys

K. Sridharan, R.D. Griffin,
R.A. Dodd, F.J. Worzala

August 1989

UWFDM-801

FUSION TECHNOLOGY INSTITUTE

UNIVERSITY OF WISCONSIN

MADISON WISCONSIN

Microstructures and Properties of Unirradiated and Irradiated High-Strength Invar Alloys

K. Sridharan*, R. D. Griffin, R. A. Dodd, F. J. Worzala*

Fusion Technology Institute
Department of Nuclear Engineering and Engineering Physics
University of Wisconsin-Madison
1500 Johnson Drive, Madison, WI 53706

*Department of Materials Science and Engineering
University of Wisconsin-Madison
1509 University Avenue, Madison, WI 53706

August 1989

UWFDM-801

Abstract

The effects of heavy-ion irradiation on two high-strength Invar alloys, INCOLOY* alloys 908 and 909, have been studied after first characterizing the alloys in the normal heat-treated condition. The unirradiated microstructures were quite different, alloy 908 consisting simply of γ' (Ni_3X) dispersed in an fcc matrix, while alloy 909 had a similar γ' dispersion together with an acicular phase and another rather massive phase at the grain boundaries and in the matrix. The chemical compositions of all phases have been determined, but the crystal structures of the acicular and massive phases in alloy 909 have not yet been determined with certainty. The mechanical properties of alloys 908 and 909 in the unirradiated conditions are comparable and the thermal expansivities are typical of Invar.

After irradiation to 8 dpa at 650°C, some of the γ' in alloy 908 had redissolved, while a high density of dislocation loops formed. Thus, even at this low damage level the microstructure was not radiation-resistant, and it was likely that there is a severe deterioration in mechanical properties. All of the phases in alloy 909 were relatively unaffected by irradiation, at least to the damage levels employed, but loops still formed in the fcc matrix. Neither alloy showed evidence for formation of voids or metastable phases.

* INCOLOY is the trademark for products of the INCO family of companies.

Introduction

The resistance of Fe-Ni-Cr austenitic alloys to radiation damage both by neutrons and charged particles has been extensively studied because of the relevance of this subject to current nuclear power technology and to the design of future fusion reactors. Most of the studies have been concerned with void swelling (including gas effects) and microstructural instability in specific alloys which were judged to be of prime interest, but for the present purposes the work of W. G. Johnston et al. (1-3) is a logical starting point.

Using 4.0 and 5.0 MeV Ni^+ beams and temperatures close to 600°C, these researchers established that in simple Fe-Ni-Cr ternary alloys there exists a pronounced minimum in swelling at intermediate nickel levels, particularly when the chromium content is low. "Invar" compositions containing roughly 35 to 50% Ni are substantially immune to void swelling up to 140 dpa. A number of more recent studies (4-8) have examined the fine-scale microstructural and microchemical changes which occur in Fe-Ni and Fe-Ni-Cr Invar alloys, and related them to the earlier void swelling observations. It has been established that a spinodal-like decomposition occurs as a result of neutron irradiation in the range 450 to 600°C, or as result of heavy ion irradiation up to 725°C. This decomposition is manifested by compositional micro-oscillations with wavelengths of hundreds of nanometers which, consequently, could be detected by energy-dispersive x-ray (EDX) analysis in the electron microscope. The oscillations result from the decomposition of the originally homogeneous Invar into regions containing roughly either 25% or 50% Ni, and the high M_S temperature of $Fe_{0.75}Ni_{0.25}$ causes these regions to transform spontaneously to martensite. The ready visibility of these martensite regions in TEM foils provides a graphic demonstration of the irradiation-enhanced decomposition of the original solid solution.

The regions which are enriched in iron (and also chromium, if present) and depleted in nickel become susceptible to void nucleation, while the nickel enriched

regions are low-swelling regions. The thermal decomposition of Fe-Ni Invar is exceedingly slow, extending over thousands of years as judged by evidence from the Santa Catherina meteorite (9), although the process is accelerated as a result of irradiation.

The interesting response of simple Invars to irradiation suggests that the irradiation behavior of more complex Invar alloys might yield information of use in the search for low-swelling stable alloys for future reactor applications.

High-Strength Invar Alloys

The obvious applicability of high-strength, creep-resistant, low thermal expansion alloys to gas turbine technology was the motivation for the development of high-strength Invar alloys during the last decade. Several such alloys are now commercially available following their evolution from the first low thermal expansion superalloy, INCOLOY alloy 903, and culminating with INCOLOY alloy 909 (10) which has a remarkable combination of tensile strength, notch rupture properties, and low thermal expansion.

The present research concentrated on INCOLOY alloys 908 and 909 (referred to as alloy 908 and alloy 909 henceforth) because, despite rather similar standard mechanical properties and thermal expansivities, there are substantial differences in the microstructures of these alloys after the recommended heat-treatment, suggesting that their responses to irradiation might also be different. The nominal compositions of these two alloys together with the standard heat treatment and selected properties are shown in Table I. All the data concerning properties were determined by the authors with the exception of Young's modulus which was provided by the International Nickel Company (INCO). The detailed results of the thermal expansion measurements are shown in Figure 1, and it is evident that these alloys do indeed possess the low expansivities characteristic of the simple Invars.

Table I. Chemical Composition (wt%), Heat Treatment and Selected Properties of INCOLOY Alloys 908 and 909

Chemical Composition*

Alloy	Fe	Ni	Co	Cr	Al	Ti	(Nb+Ta)	C	Si	Mn	S
INCO 908	40.6	49.76	--	3.83	1.04	1.58	2.99	0.01	0.14	0.04	0.001
INCO 909	41.41	38.93	12.73	--	0.06	1.61	4.93	0.01	0.3	0.02	0.001

Heat Treatment*

982°C for 1 hour, Air Cool/ 718°C for 8 hours, Furnace Cool/ 621°C for 8 hours, Air Cool

Selected Properties

Property	INCO 908	INCO 909
Ultimate Tensile Strength (MPa)	1.34×10^3	1.27×10^3
Yield Strength (0.2% offset, MPa)	1.06×10^3	1.03×10^3
Elongation (%)	14	15
Hardness (R_C)	45	43
Inflection Temperature (°C)	270	420
Average Thermal Expansion (/°C) (from 25°C to inflection temp.)	7.4×10^{-6}	7.1×10^{-6}
Average Thermal Expansion (/°C) (from 25°C to 600°C)	11.6×10^{-6}	9.1×10^{-6}
Young's Modulus (GPa)*	166	159

*Data supplied by International Nickel Company.

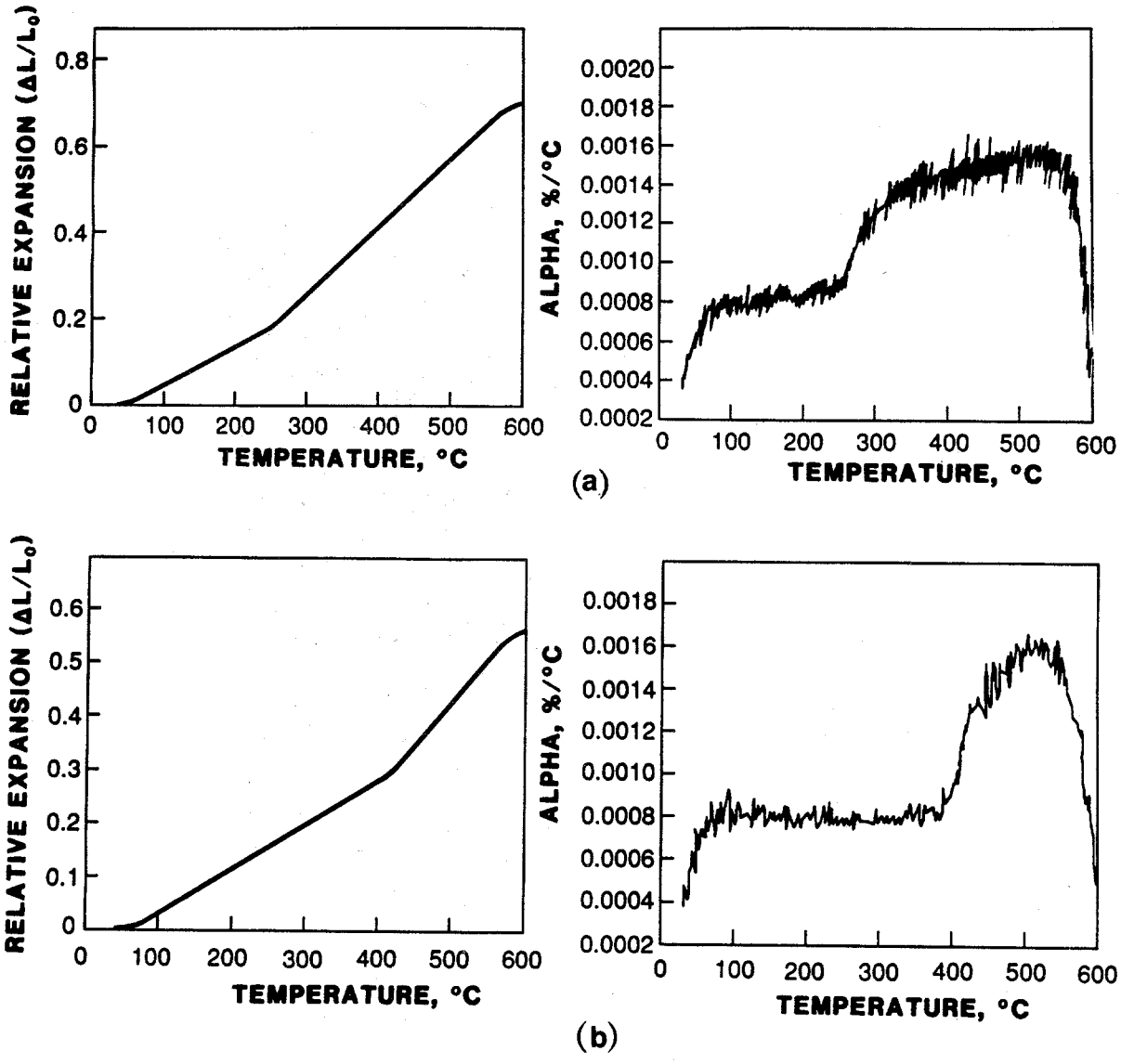

Figure 1. Thermal expansion characteristics of alloys (a) 908 and (b) 909.

Characteristics of the Unirradiated Alloys

The results of differential thermal analysis (DTA) of the solutionized and quenched alloys 908 and 909 are shown in Figure 2. In both cases the heating (and cooling) rate was 10°C min^{-1}. The analysis for alloy 908 was straightforward; gamma prime precipitated at just above 600°C and redissolved at about 820°C. There was no evidence for any other reaction, a fact which agreed with the microstructural studies. In alloy 909, γ' formed at about 775°C and another precipitate - acicular, based on TEM observations - formed at 825°C (heating curve 1). Evidently, the kinetics of the acicular precipitation were slow because on cooling and reheating after the initial heating (heating curve 2), a substantial acicular precipitate peak was again observed, although there was no evidence for additional γ' precipitation.

The general unirradiated microstructures of heat-treated alloys 908 and 909, as determined by TEM, are shown in Figure 3. The structure of alloy 908 consisted of a uniform distribution of grains of the fcc matrix, with an even dispersion of γ', in agreement with the DTA data. The γ' was not well resolved in the low-magnification micrograph of Figure 3, but is readily apparent in Figure 4. The accompanying selected area diffraction pattern shows the γ' diffraction patterns clearly (along with the background matrix diffraction pattern), the orientation relationship between them being $100_{\{matrix\}} \parallel 100_{\{gamma\ prime\}}$. The precipitates were successfully extracted via carbon extraction replicas, and their compositions were determined by EDX in a HB 501 dedicated STEM, the spectrum also being shown in Figure 4. The quantitative EDX data for all precipitates in both alloys 908 and 909 are shown in Table II. The high concentration of silicon in the 908 γ' phase is noteworthy because the bulk composition contained only 0.14% Si. In contrast, the 909 bulk composition contained 0.3% Si, while the alloy 909 γ' contained only 1.48% Si.

The microstructure of alloy 909 was quite complex as evidenced by Figure 3. As in alloy 908, the γ' is not well resolved at this low magnification but long acicular

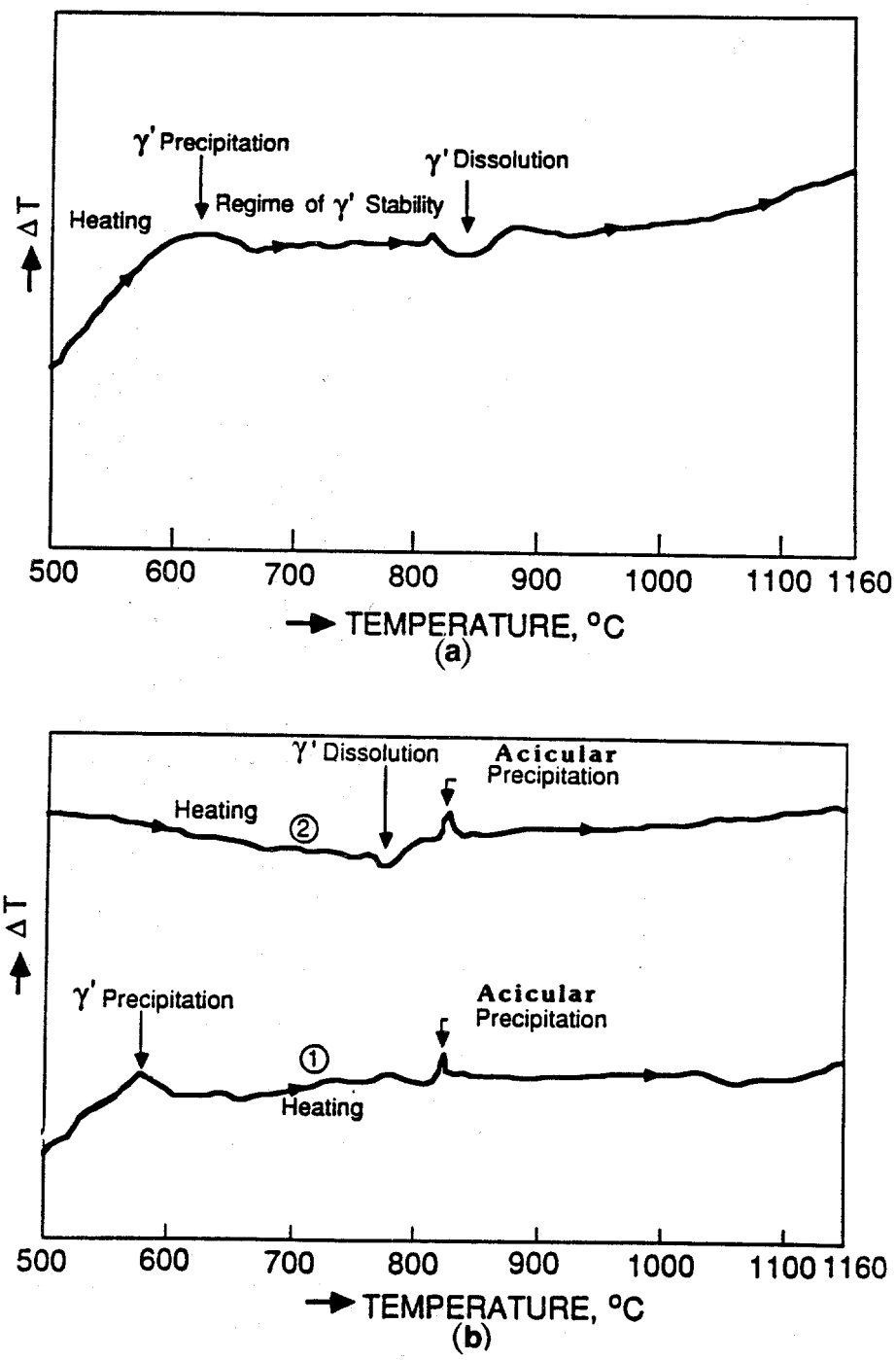

Figure 2. Differential thermal analysis results showing the temperature regime of stability of precipitates for (a) 908 and (b) 909.

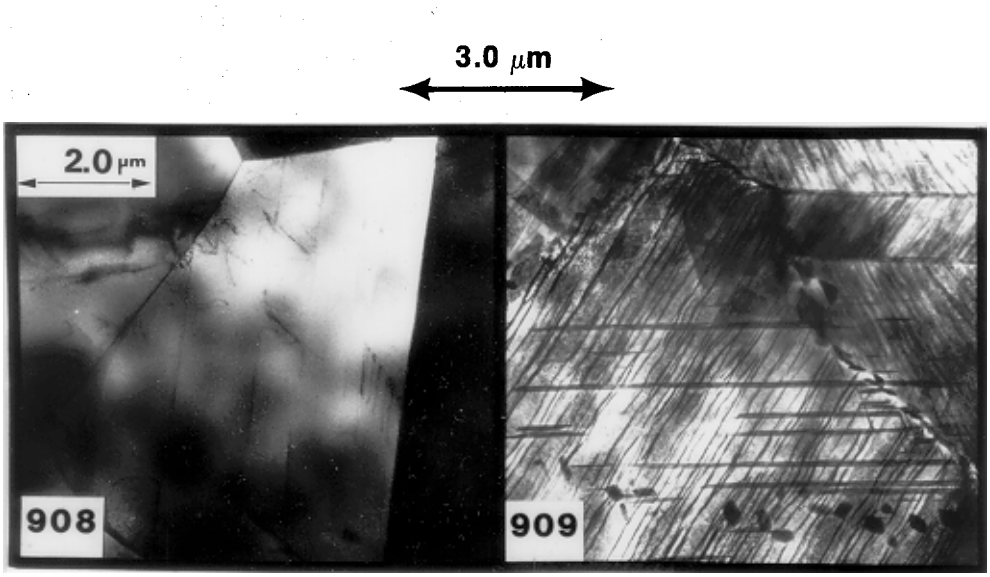

Figure 3. General microstructure of alloys 908 and 909.

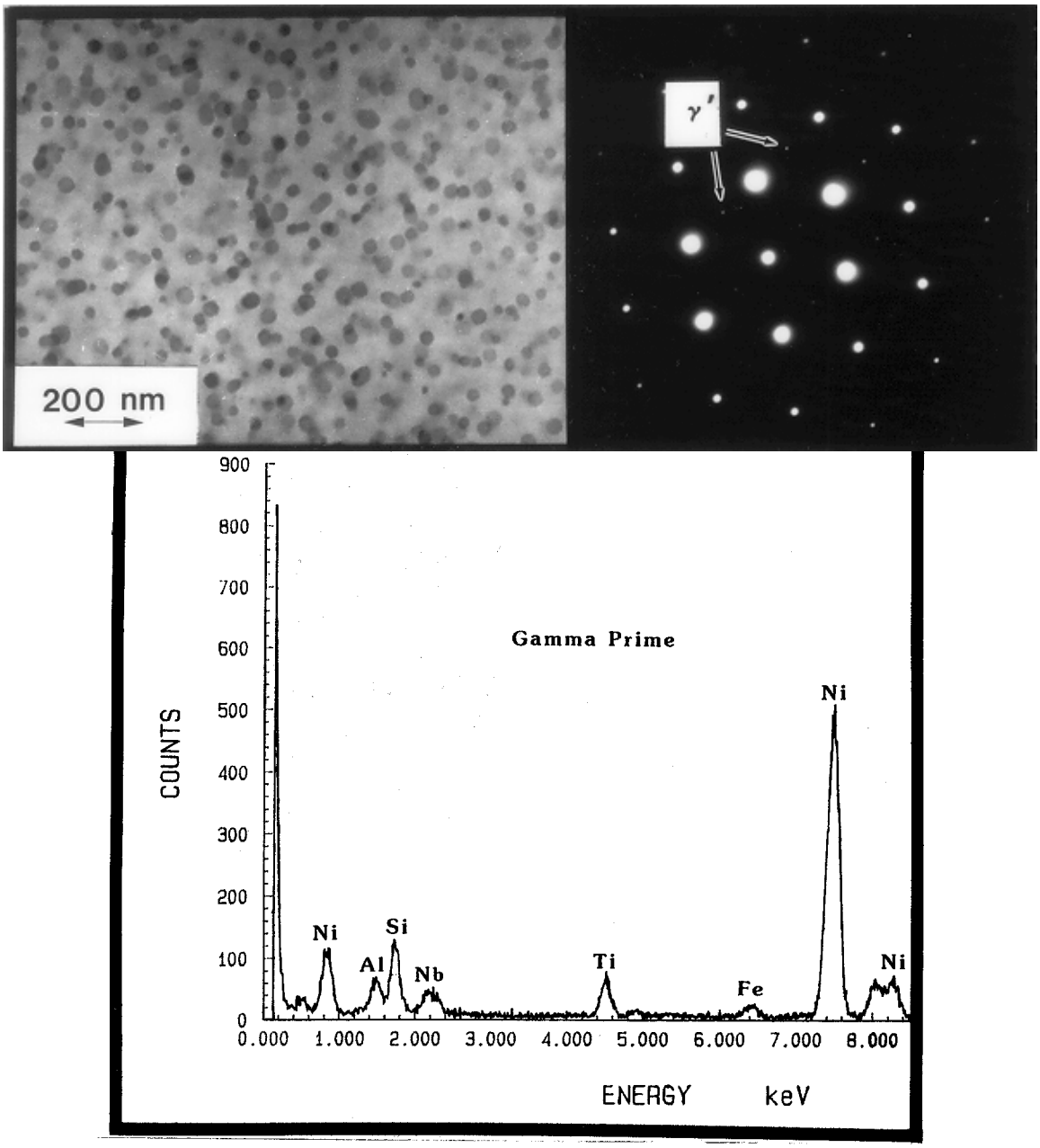

Figure 4. Microstructural, diffraction and EDX data for gamma prime precipitates in alloy 908.

Table II. Chemical Analysis (wt%) of Precipitates Observed in INCOLOY Alloys 908 and 909

Alloy/Precipitate	Fe	Ni	Nb	Co	Al	Si	Ti
908/gamma prime	2.8	71.3	7.3	--	4.4	8.0	6.2
909/gamma prime	5.9	57.0	18.4	9.2	--	1.5	8.0
909/acicular	17.6	22.3	40.5	5.3	1.0	2.3	11.0
909/blocky grain boundary and matrix	13.6	34.1	36.6	9.4	0.8	3.8	1.7

precipitates and massive (or blocky) grain boundary and matrix particles are quite apparent. The morphology of the γ' is seen clearly in Figure 5, and, as noted, the most interesting difference in the γ' in the two alloys was the variation in silicon content. The composition of the acicular precipitates in alloy 909 is listed in Table II, and the microstructure and EDX spectrum in Figure 6. Once again, the EDX data refers to extracted precipitates examined in a HB 501 STEM, so the quoted composition is reasonably exact. These precipitates did not grow across grain boundaries, and they appear to have a specific orientation relationship with the matrix. However, satisfactory electron diffraction patterns for these precipitates have not yet been obtained, so that their structure and orientation relationship to the matrix currently are unknown. Finally, the morphological, diffraction and EDX evidence for the grain boundary and massive matrix precipitates in alloy 909 is shown in Figures 7 and 8. The similarity of the EDX data (see Table II) suggests that there was no difference between these grain boundary and matrix precipitates but again the electron diffraction data is not yet conclusive. However, the phase is cubic with a_o= 0.67 nm.

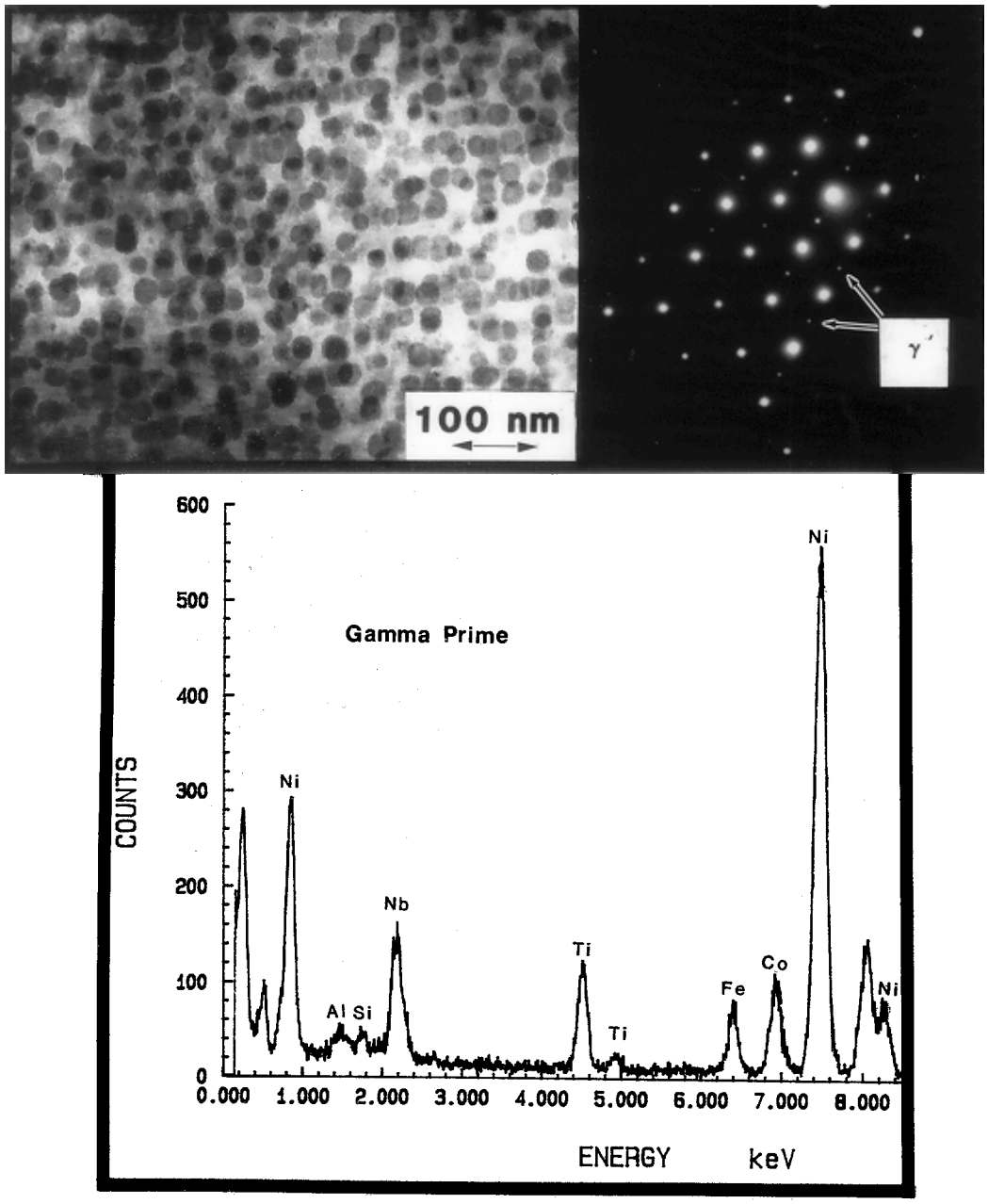

Figure 5. Microstructural, diffraction and EDX data for gamma prime precipitates in alloy 909.

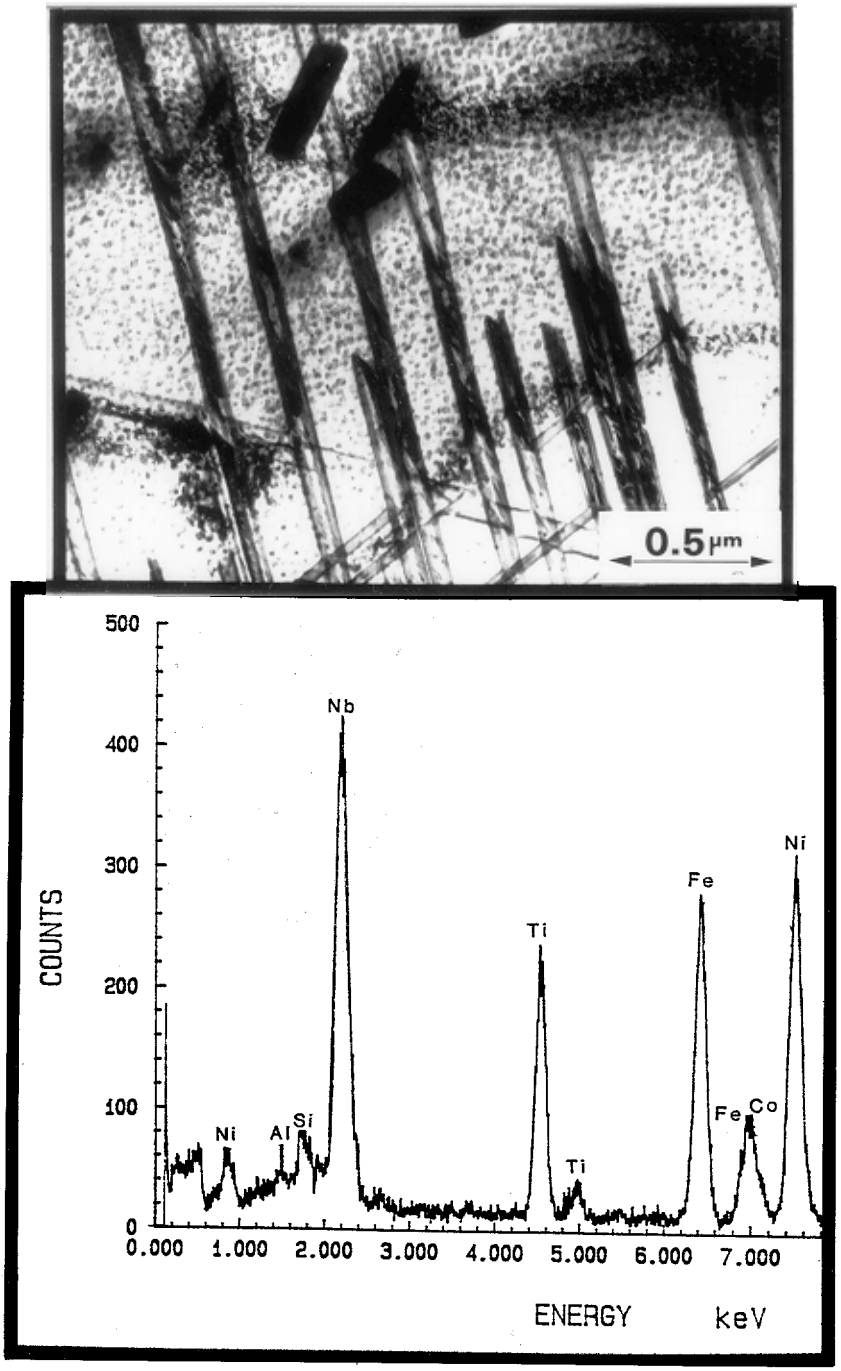

Figure 6. Microstructural and EDX results for acicular precipitates in alloy 909.

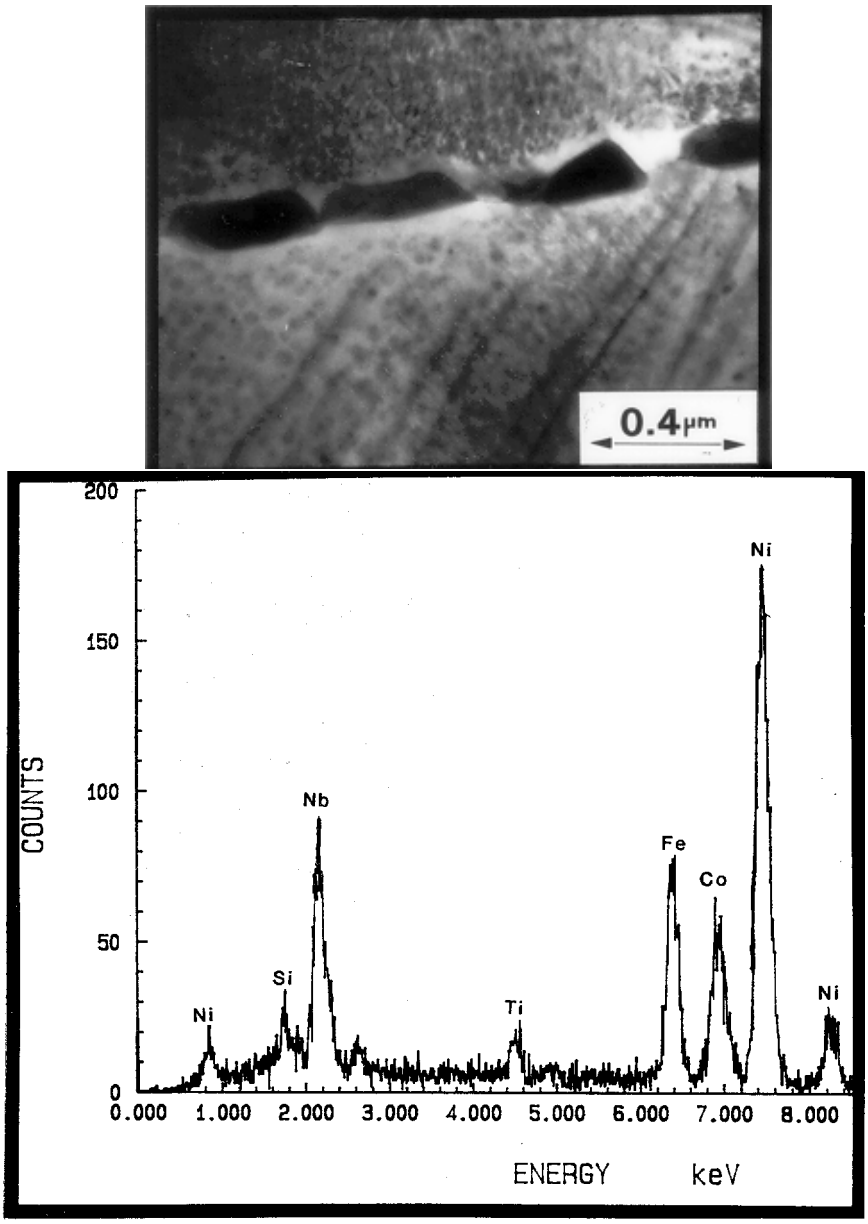

Figure 7. Microstructural and EDX data for grain boundary precipitates in alloy 909.

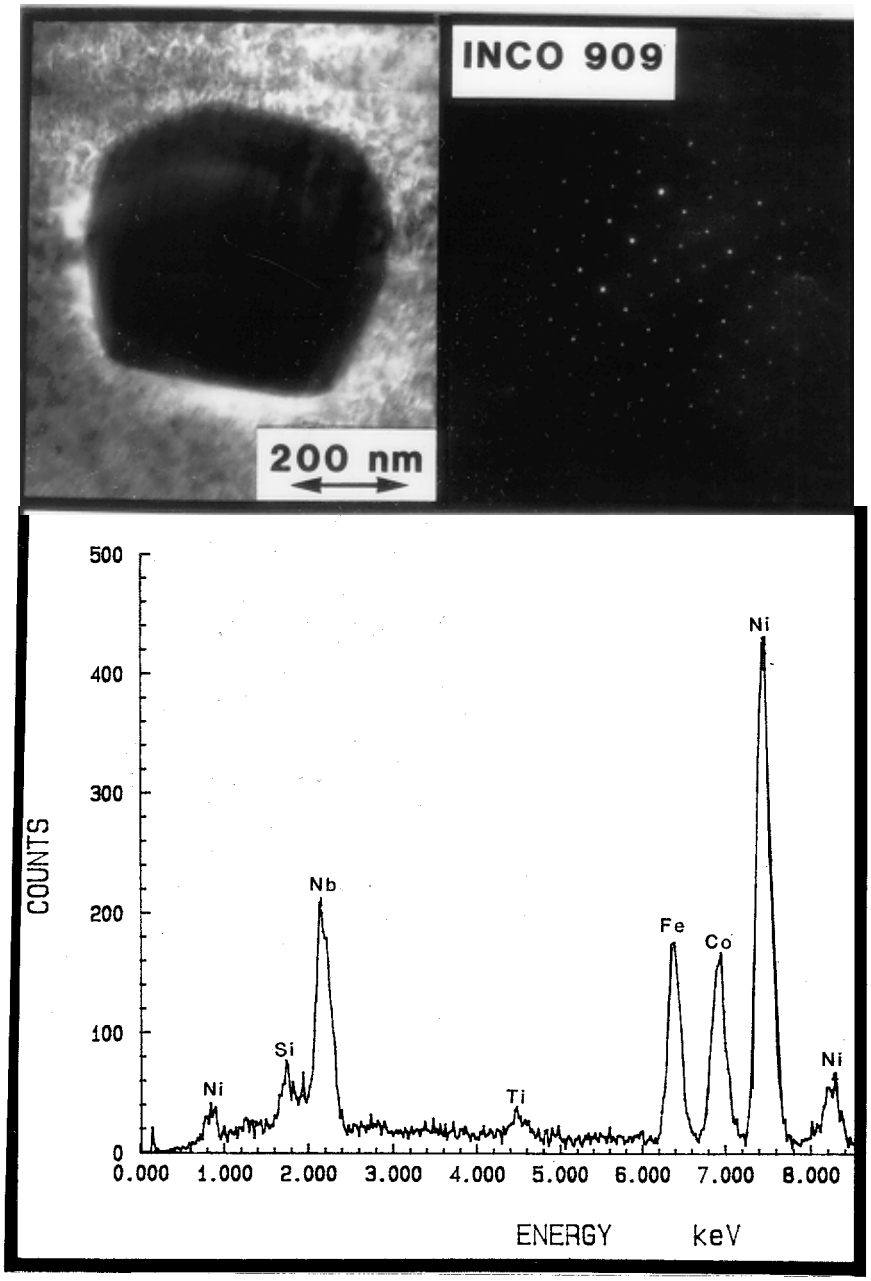

Figure 8. Microstructural, diffraction and EDX data for massive precipitates in the alloy 909 matrix.

A recent, detailed study of alloy 909 by Heck et al. (11) has indicated that the crystal structure of the acicular precipitates may be distorted hexagonal or fcc. An ε-phase with a blocky, angular morphology and a DO_{19} hexagonal superlattice structure has been observed to precipitate at the grain boundaries and the matrix while two and four layered hexagonal Laves phases with similar morphology have also been identified at the grain boundaries.

Irradiation Effects on INCOLOY Alloys 908 and 909

Heat treated 3 mm disks of both alloys were irradiated at 650°C with 3.6 MeV Fe^+ to a peak dpa of ~20. The depth profiles of displacement damage and implanted ion concentration calculated by a Monte Carlo code, TAMIX (12), are shown in Figure 9. Some specimens were irradiated simply as described above, while others were co-implanted with helium at 0.2 to 0.4 MeV to give an approximately uniform helium concentration of about 10 appm up to depths of about 500 nm. Because of this limited helium range, all irradiated foils were simply back-thinned to provide a foil corresponding to ~8 dpa.

The effect of helium in nucleating voids is well known, but no voids were observed in any of the irradiated alloys, with or without helium present. However, a dose of <10 dpa is much too low to permit a definitive statement regarding the swelling propensities of the alloys, and so attention was concentrated on possible modification of the precipitate microstructures. Looking first at alloy 908, the microstructure changed profoundly even at the low irradiation dose employed, as seen by comparing Figures 10a and 4. The γ' is not readily evident after irradiation and, instead, a high density of dislocation loops formed. It cannot be said that the γ' was completely dissolved because electron diffraction evidence showed its continued presence in some regions of the foil, i.e. a γ' spot pattern could occasionally be obtained even though the phase was not visible with conventional bright field imaging. Nevertheless, these observations strongly suggested that the mechanical properties of alloy 908 cannot be

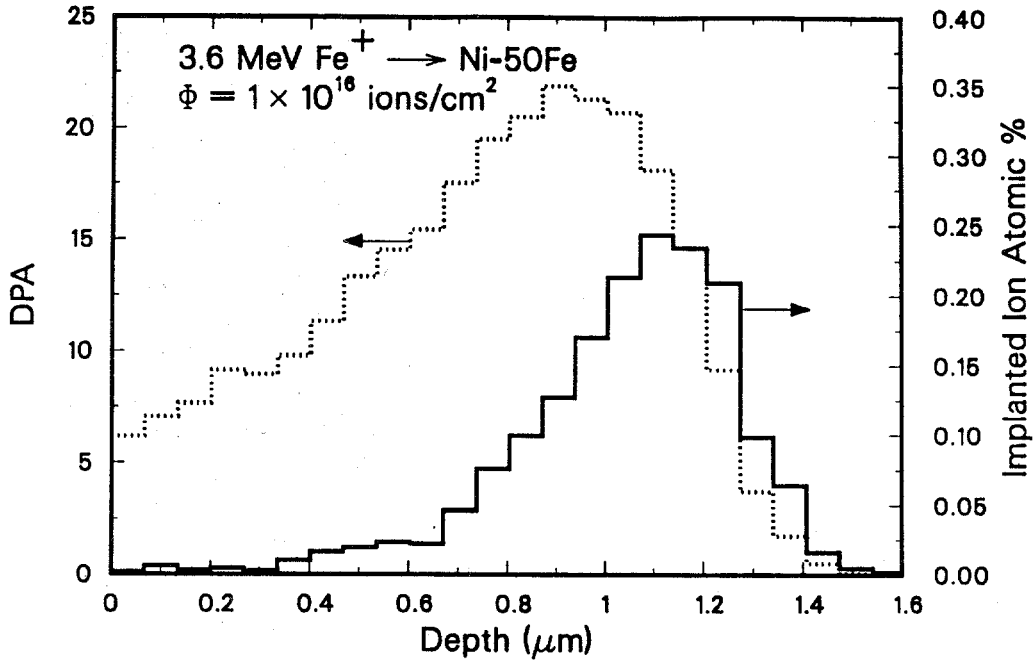

Figure 9. Calculated damage profile of 3.6 MeV Fe^+ and ranges of incident Fe^+ in Ni-50Fe.

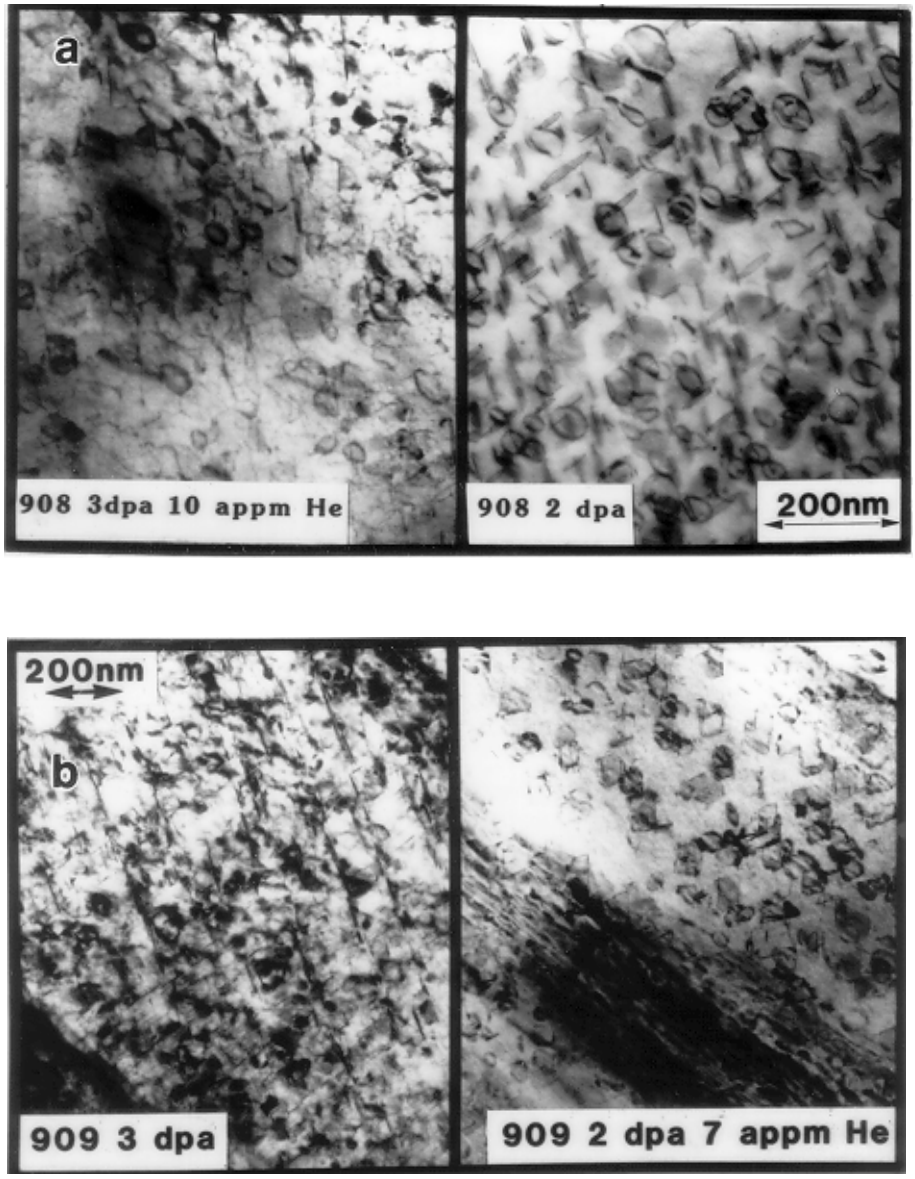

Figure 10. Microstructure after irradiation at 650°C to 8 dpa for alloys (a) 908 and (b) 909.

maintained in a radiation environment at 650°C despite the DTA (and TEM) evidence for the thermal stability of the alloy to considerably higher temperatures, in the unirradiated condition. The presence of helium had no obvious effect on the precipitate microstructure.

The γ' in alloy 909 was much more stable to irradiation than the γ' in alloy 908, at least at the temperature and damage level employed, despite the DTA evidence that this phase in alloy 909 was solutionized at a lower temperature. Undoubtedly, a number of factors may affect the resolutionizing kinetics so the reasons for the observation remain unknown. As in alloy 908, dislocation loops were formed during irradiation (see Figure 10b), and the additive effects of γ' and loop strengthening suggested that the mechanical properties of this alloy may have improved rather than deteriorated as a result of the irradiation. The acicular and blocky precipitates were not noticeably affected by irradiation but in any case they probably represent only a minor secondary source of hardening.

Conclusions

The heat treated but unirradiated microstructures of alloys 908 and 909 had a fundamental similarity, namely a high density of γ' precipitates in an fcc matrix. This phase provided the major source of strengthening in both alloys. The γ' was the only precipitated phase in alloy 908, but alloy 909 also contained acicular precipitates in the fcc matrix and a blocky or massive phase which occurred in the grain boundaries and within the fcc matrix. Thus alloy 908 was overwhelmingly a two-phase alloy, while alloy 909 contained four identifiable phases. The precipitated phases in alloy 909 could be distinguished on grounds of morphology and chemical composition, but, except for γ', the diffraction evidence was incomplete so that the two phases cannot be completely described. There was, however, evidence that the massive precipitates were fcc or diamond cubic with a lattice parameter of $a_0 \approx 0.67$ nm.

The simple microstructure of alloy 908 was quite unstable as a result of ion irradiation to ~8 dpa at 650°C, i.e. the γ' dissolved. The inevitable concomitant deterioration of mechanical properties suggests that this alloy is unsuitable as a reactor constructional material. Under similar conditions, the alloy 909 exhibited little microstructural change, so that this alloy, or others of comparable microstructure may be worth investigating further. Of course, the damage levels employed were far too low to permit an assessment of swelling resistance in either alloy.

Acknowledgements

The authors are grateful to Dr. S.J. Zinkle for arranging the ion irradiations at Oak Ridge National Laboratory, and thank the personnel of the Argonne National Laboratory for assistance in performing the thermal expansion measurements at that institution. The authors would like to thank the International Nickel Company for supplying the alloys. One of the authors (RDG) acknowledges the support of a NORCUS fellowship during the period of the research.

References

1. W.G. Johnston, T. Lauritzen, J.H. Roslowski and A.M. Turkalo, Radiation Damage in Metals, Eds. N.L. Peterson and S.D. Harkness, ASM, Cleveland, OH, 1976, pp. 227-266.

2. W.G. Johnston, J.H. Roslowski, A.M. Turkalo, and T. Lauritzen, J. Nucl. Mater., 1974, 54, pp. 24-40.

3. J.F. Bates and W.G. Johnston, Radiation Effects in Breeder Reactor Structural Material, Eds. M.L. Bleisberg and J.W. Bennett, Trans. Met. Soc. AIME, 1977, pp. 625-644.

4. H.R. Brager and F.A. Garner, Optimizing Materials for Nuclear Applications, Eds. F.A. Garner, D.S. Gelles and F.W. Wiffen, Trans. Met. Soc. AIME, 1985, pp. 141-166.

5. H.R. Brager and F.A. Garner, Effects of Radiation on Materials, Twelfth International Symposium, STP 870, American Society for Testing and Materials, 1985, pp. 139-150.

6. F.A. Garner, H.R. Brager, M.L. Hamilton, R.A. Dodd, and D.L. Potter, Radiation Effects, 1986, 101, pp. 37-53.

7. F.A. Garner, H.R. Brager, R.A. Dodd and T. Laurtizen, Nuclear Instr. and Methods in Nuclear Research, 1986, B16, pp. 244-255.

8. R.A. Dodd, F.A. Garner, J-J. Kai, T. Lauritzen and W.G. Johnston, Radiation-Induced Changes in Microstructure: Thirteenth International Symposium, STP 955, ASTM, 1985, pp. 788-804.

9. F.A. Garner, H.R. Brager and J.M. McCarthy, Radiation-Induced Changes in Microstructure: Thirteenth International Symposium, STP 955, ASTM, 1987, pp. 775-787.

10. D. Smith, J. Smith and S. Floreen, Superalloys 1984, TMS-AIME, 1984, pp. 591-600.

11. K.A. Heck, et al., Superalloys 1988, TMS-AIME, p. 151-160.

12. S. Han and G. L. Kulcinski, Fusion Reactor Materials, DOE/ER-0313/2, 1987, pp. 105-109.